

Testing black holes in non-linear electrodynamics from the observed quasi-periodic oscillations

Indrani Banerjee*¹

¹Department of Physics and Astronomy, National Institute of Technology, Rourkela-769008, India

Abstract

Quasi-periodic oscillations (QPOs), in particular, the ones with high frequencies, often observed in the power spectrum of black holes, are useful in understanding the nature of strong gravity since they are associated with the motion of matter in the vicinity of the black hole horizon. Interestingly, these high frequency QPOs (HFQPOs) are observed in commensurable pairs, the most common ratio being 3:2. Several theoretical models are proposed in the literature which explain the HFQPOs in terms of the orbital and epicyclic frequencies of matter rotating around the central object. Since these frequencies are sensitive to the background spacetime, the observed HFQPOs can potentially extract useful information regarding the nature of the same. In this work, we investigate the role of regular black holes with a Minkowski core, which arise in gravity coupled to non-linear electrodynamics, in explaining the HFQPOs. Regular black holes are particularly interesting as they provide a possible resolution to the singularity problem in general relativity. We compare the model dependent QPO frequencies with the available observations of the quasi-periodic oscillations from black hole sources and perform a χ^2 analysis. Our study reveals that most QPO models favor small but non-trivial values of the non-linear electrodynamics charge parameter. In particular, black holes with large values of non-linear electrodynamics charge parameter are generically disfavored by present observations related to QPOs.

1 Introduction

The theorems of Hawking and Penrose [1] state that black hole (henceforth as BH) singularities are an unavoidable feature of general relativity. However, it is believed that spacetime singularities should not exist in Nature and a suitable theory of quantum gravity can address this issue. In this regard various quantum gravity models have been put forward [2–10]. In the absence of a well established quantum gravity model one can address the black hole singularity problem classically by studying black holes with regular cores. Such black holes have horizons such that their metric and curvature invariants are non-singular at all points in spacetime. Motivated by quantum arguments [11–13] it was proposed that the central region of the black hole at $r \simeq 0$ should be de-Sitter like which was studied extensively [14–16]. These works propound that quantum fluctuations prevent the unlimited increase of spacetime curvature during the stellar collapse process giving rise to black holes with regular cores.

The first regular black hole solution with a de-Sitter core was proposed by Bardeen [17] which turns out to be a solution of Einstein's equations coupled to non-linear electrodynamics. Later Ayon-Beato

*banerjeein@nitrkl.ac.in

and Garcia [18] explained that the physical source that gives rise to the Bardeen solution corresponds to the gravitational field of a nonlinear magnetic monopole of a self-gravitating magnetic field. Several other regular black hole solutions of gravity coupled to non-linear electrodynamics have been obtained later [18–20]. Since then there has been a lot of research in the direction of investigating regular black holes [21–28].

In this work, we study a class of regular black hole in non-linear electrodynamics with an asymptotically Minkowski core. Such a metric arises as the solution of Einstein’s equations with an anisotropic fluid resembling the Maxwell stress tensor far from the source [29]. The electric field from such a source asymptotically resembles the Coulomb field, is bound at all distances, and the corresponding geometry is like that of Reissner-Nordstrom (RN) metric far from the source. The motivation for exploring such black hole solution stems from the fact that the mass function has an exponential convergence factor which makes the quantum gravity model finite to all orders upto the Planck scale [30]. Further, study of a finite quantum gravity is important as it can address the cosmological constant problem [31] and can eliminate the divergences arising in flat space quantum field theories.

Since black holes observed in nature are in general rotating the stationary and axi-symmetric counterpart of the aforesaid regular solution with Minkowski core have been worked out by applying the Newman-Janis algorithm [32] and other methods [33–35]. These algorithms also enable one to derive regular black hole solutions inspired from non-commutative geometry with a regular de-Sitter toroidal core [36]. Since we will be interested in exploring the aforesaid metric in the context of astrophysical observations we work with the rotating counterpart in this work [37]. As expected, the rotating solution resembles the Kerr-Newman metric far from the source. When the radiating counterpart of this spacetime is considered one obtains generalization of Carmeli’s spacetime as well as Vaidya’s spacetime in suitable limits.

In this work our goal is to extract signatures of the non-linear electrodynamics charge parameter from the quasi-periodic oscillations (QPOs) observed in the power density spectrum of black holes. QPOs generally appear as peaks in the power spectrum of Low-Mass X-ray binaries (LMXBs) which includes black hole and neutron star sources. Although rare, certain active galactic nuclei (AGNs) also exhibit QPOs in the power spectrum. It is believed that QPOs, in particular, the ones with high frequencies (henceforth referred as HFQPOs) encapsulate information regarding the nature of strong gravity associated with these compact objects and hence these can serve as effective tools to study the alternatives to general relativity [38, 39]. The QPO frequencies are inversely proportional to the mass of the compact objects, such that for neutron stars HFQPOs \sim kHz, for stellar-mass black holes they are \sim hundreds of Hz while for supermassive black holes they are in the mHz order [40, 41]. The order of magnitude of the HFQPOs can be directly attributed to the timescales associated with the motion of matter close to the compact objects. This can be directly seen from the fact that the dynamical time scale $t_d \sim r^3/GM \sim$ milli-seconds for neutron stars and stellar-mass BH sources when $r < 10 r_g$ is considered [40–43]. This was predicted in the 1970s which later received confirmation with the launch of NASA’s Rossi X-Ray Timing Explorer satellite. Thus, QPOs provide unique opportunity to explore the nature of strong gravity and dense matter. Since we intend to investigate the nature of strong gravity, i.e. to study the role of the NED charge parameter in explaining the observed QPOs we will concentrate only on black hole sources in this work.

The paper is organized in the following way: In Section 2 we discuss the black hole solution considered in this work which arises when gravity is coupled to non-linear electrodynamics. The motion of test particles in such a spacetime is studied in Section 3 and the dependence of the epicyclic frequencies on the background spacetime is derived. Section 4 is dedicated in reviewing the various theoretical models proposed to explain the observed QPOs. In Section 5 we compare the various model dependent QPO frequencies with observations and perform a χ^2 analysis to derive the observationally favored NED charge parameter. We conclude with a summary of our results and discuss some avenues for future work in

Section 6.

2 Regular rotating black holes in non-linear electrodynamics with a Minkowski core

In this work we consider regular black holes in non-linear electrodynamics with an asymptotically Minkowski core. The action corresponding to non-linear electrodynamics coupled to Einstein gravity is given by [13, 18, 44–47],

$$S = \int d^4x \sqrt{-g} \left(\frac{\mathcal{R}}{16\pi} - \frac{L(F)}{4\pi} \right) \quad (1)$$

where \mathcal{R} is the Ricci scalar and $L(F)$ is the Lagrangian density associated with non-linear electrodynamics such that $F = F^{\mu\nu} F_{\mu\nu}/4$ is the Faraday invariant and $F_{\mu\nu} = \partial_\mu A_\nu - \partial_\nu A_\mu$ is the electromagnetic field strength tensor with A_μ the gauge field. The Maxwell theory is retrieved in the weak field limit when $L(F) = F$. Varying the action with respect to the metric yields the Einstein's equations with $L(F)$ as the source,

$$G_{\mu\nu} = 2(L_F F_\mu^\sigma F_{\nu\sigma} - g_{\mu\nu} L(F)) \quad (2)$$

where $L_F = \frac{\partial L}{\partial F}$ and $G_{\mu\nu}$ is the Einstein tensor. On the other hand, varying the action with respect to A_μ yields the equation of motion corresponding to non-linear electrodynamics,

$$\{L_F F^{\mu\nu}\}_{;\mu} = 0 \quad (*F^{\mu\nu})_{;\nu} = 0 \quad (3)$$

where $*F^{\mu\nu} = \epsilon^{\mu\nu\alpha\beta} F_{\alpha\beta}$ is the Hodge-dual of $F^{\mu\nu}$. When the Lagrangian density corresponding to non-linear electrodynamics is considered to be,

$$L(F) = F e^{-\alpha(2q^2 F)^{1/4}} \quad (4)$$

with $\alpha = qc^2/(2G\tilde{\mathcal{M}})$ (q being the charge and $\tilde{\mathcal{M}}$ the mass of the black hole), the static, spherically symmetric and asymptotically flat solution of Eq. (2) assumes the form,

$$ds^2 = -\left(1 - \frac{2\tilde{m}(r)}{r}\right) dt^2 + \frac{dr^2}{\left(1 - \frac{2\tilde{m}(r)}{r}\right)} + r^2(d\theta^2 + \sin^2\theta d\phi^2) \quad (5)$$

with the mass function

$$\tilde{m}(r) = \tilde{\mathcal{M}} e^{-\kappa/r} \quad (6)$$

where $\kappa = \frac{q^2 c^2}{2G\tilde{\mathcal{M}}}$ has dimensions of length. The above spacetime has two horizons [44, 48]. The outer horizon corresponds to $r_+ = 2\tilde{\mathcal{M}} e^{W_0(-\frac{\kappa}{\tilde{\mathcal{M}}})}$ while the inner horizon corresponds to $r_- = 2\tilde{\mathcal{M}} e^{W_{-1}(-\frac{\kappa}{\tilde{\mathcal{M}}})}$, where W_0, W_{-1} corresponds to the Lambert W function. When $r = \kappa$ the two horizons merge resulting in the extremal black hole scenario.

The above metric arises from the solution of Einstein's equations with the source,

$$\begin{aligned}
T_0^0 &= -\rho(r) = \frac{-\tilde{M}\kappa}{4\pi r^4} e^{-\kappa/r}; \\
T_1^1 &= -\rho(r) = \frac{-\tilde{M}\kappa}{4\pi r^4} e^{-\kappa/r}; \\
T_2^2 &= T_3^3 = \frac{\tilde{M}\kappa}{4\pi r^4} \left(1 - \frac{\kappa}{2r}\right) e^{-\kappa/r}
\end{aligned} \tag{7}$$

The energy density and pressure described by Eq. (7) tends to zero as $r \rightarrow \infty$ and are non-singular at $r = 0$. We further note that the above energy momentum tensor satisfies the weak energy condition and goes over to the Maxwell stress tensor far from the horizon [49].

Since black holes in astrophysics are in general rotating, studying rotating black hole solutions of the above Einstein's equations are more important. Such a solution is generated by applying the Newman Janis algorithm [32–35] and turns out to be

$$\begin{aligned}
ds^2 &= -\left(1 - \frac{2\tilde{m}(r)r}{\tilde{\Sigma}}\right) dt^2 - \frac{4a\tilde{m}(r)r}{\tilde{\Sigma}} \sin^2 \theta dt d\phi + \frac{\tilde{\Sigma}}{\Delta} dr^2 \\
&\quad + \tilde{\Sigma} d\theta^2 + \left(r^2 + a^2 + \frac{2\tilde{m}(r)ra^2}{\tilde{\Sigma}} \sin^2 \theta\right) \sin^2 \theta d\phi^2
\end{aligned} \tag{8}$$

where,

$$\tilde{\Sigma} = r^2 + a^2 \cos^2 \theta, \quad \Delta = r^2 + a^2 - 2\tilde{m}(r)r \tag{9}$$

and $\tilde{m}(r)$ is the mass function mentioned in Eq. (6) such that $\lim_{r \rightarrow \infty} \tilde{m}(r) = \tilde{M}$ and a is the spin parameter of the black hole. Since it is computationally easier to handle dimensionless quantities we scale κ and r in Eq. (6) by the gravitational radius $r_g = GM/c^2$. Thus the dimensionless metric parameters correspond to the squared charge to mass ratio $k = \kappa/r_g = \frac{q^2 c^4}{2G^2 M^2}$ and the spin parameter $a \equiv a/r_g$.

The above metric goes over to the Kerr-Newman spacetime when $r \gg \kappa$. It is important to note that the above black hole solution does not have the curvature singularity at $r = 0$ and has an asymptotically Minkowski core. In such a situation the energy density $\rho(r) \rightarrow 0$ as $r \rightarrow 0$ unlike a de-Sitter core where the energy density becomes constant at the core. It turns out that the curvature tensor and invariants in the above spacetime are considerably simpler than the Bardeen metric and has several physically interesting features defined by the Lambert W function [49–56].

In the absence of nonlinear electrodynamics when $\kappa = 0$ the above black hole solution reduces to the Kerr metric. The event horizon of the above metric is obtained by solving for the roots of $g^{rr} = \Delta = 0$ which gives,

$$r^2 + a^2 - 2re^{-k/r} = 0 \tag{10}$$

For the metric in Eq. (8) to represent a black hole real, positive horizons must be present. This sets the physically allowed range of k to $0 \lesssim k \lesssim 0.7$ [57].

In the next section we discuss the derivation of the epicyclic frequencies of the accreting test particles in the above spacetime.

3 Epicyclic frequencies of test particles in a stationary axisymmetric black hole spacetime

This section investigates motion of massive test particles around a rotating black hole described by a stationary, axisymmetric spacetime whose metric is given by,

$$ds^2 = g_{tt}dt^2 + 2g_{t\phi}dtd\phi + g_{\phi\phi}d\phi^2 + g_{rr}dr^2 + g_{\theta\theta}d\theta^2, \quad (11)$$

We assume that the above spacetime has reflection symmetry such that $g_{\mu\nu}(r, \theta) = g_{\mu\nu}(r, -\theta)$. Stationarity and axisymmetry implies ∂_t and ∂_ϕ are Killing vectors such that the specific energy E and the specific angular momentum L of the test particles are conserved. The test particles moving in such a spacetime move in an effective potential given by,

$$V(r, \theta) = (g^{tt} - 2lg^{t\phi} + l^2g^{\phi\phi}) \quad (12)$$

which can be obtained from the invariance of the rest mass of the test particles such that,

$$\dot{r}^2g_{rr} + \dot{\theta}^2g_{\theta\theta} + E^2V(r, \theta) = -1 \quad (13)$$

where $l = L/E$ is the impact parameter in Eq. (12). If we consider circular orbits in the equatorial plane the above equation reduces to

$$E^2V(r_0, \pi/2) = -1 \quad (14)$$

where the radius of the circular orbit is denoted by r_0 . The radial Euler-Lagrange equation leads to a quadratic equation for the angular frequency

$$g_{tt,r} + 2\Omega g_{t\phi,r} + \Omega^2 g_{\phi\phi,r} = 0. \quad (15)$$

which when solved gives

$$\Omega = \frac{-g_{t\phi,r} \pm \sqrt{g_{t\phi,r}^2 - g_{tt,r}g_{\phi\phi,r}}}{g_{\phi\phi,r}} \quad (16)$$

where \pm sign represents prograde and retrograde orbits respectively. We next consider slight perturbations in the motion of the test particle from the circular orbit and the equatorial plane which are denoted by,

$$r(t) \simeq r_0 + \delta r_0 e^{i\omega_r t}; \quad \theta(t) \simeq \frac{\pi}{2} + \delta\theta_0 e^{i\omega_\theta t}. \quad (17)$$

where ω_r and ω_θ correspond to radial and vertical epicyclic frequencies respectively. Substituting Eq. (17) in Eq. (13) and Taylor expanding $U(r, \theta)$ about $r = r_0$ and $\theta = \pi/2$ we get,

$$-\delta r_0^2 \omega_r^2 (u^t)^2 g_{rr} - \delta\theta_0^2 \omega_\theta^2 (u^t)^2 g_{\theta\theta} + E^2 \left[V(r_0, \pi/2) + \frac{1}{2} \frac{\partial^2 V}{\partial r^2} \Big|_{r=r_0, \theta=\pi/2} \delta r^2 + \frac{1}{2} \frac{\partial^2 V}{\partial \theta^2} \Big|_{r=r_0, \theta=\pi/2} \delta \theta^2 \right] = -1 \quad (18)$$

In Eq. (18) we retain terms upto quadratic order such that the motion in the radial and the vertical direction are uncoupled. Using Eq. (14) in Eq. (18) and by equating the coefficients of δr^2 and $\delta \theta^2$ on

both sides of Eq. (18) we obtain radial and the vertical epicyclic frequencies of the test particles in the above spacetime which are respectively given by,

$$\omega_r^2 = \frac{c^6}{G^2 \tilde{M}^2} \frac{(g_{tt} + \Omega g_{t\phi})^2}{2g_{rr}} \frac{\partial^2 V}{\partial r^2} \Big|_{r=r_0, \theta=\pi/2} \quad (19)$$

$$\omega_\theta^2 = \frac{c^6}{G^2 \tilde{M}^2} \frac{(g_{tt} + \Omega g_{t\phi})^2}{2g_{\theta\theta}} \frac{\partial^2 V}{\partial \theta^2} \Big|_{r=r_0, \theta=\pi/2} \quad (20)$$

In Eq. (20) the radial and vertical epicyclic frequencies are multiplied by the factor $(c^6/G^2 \tilde{M}^2)$ so that they have dimensions of frequency squared. We note that these are functions of the black hole mass \tilde{M} , the radius at which these oscillations are generated r_{em} and the metric parameters k and a .

Table 1 below enlists some BH sources where QPOs have been discovered. We are chiefly interested in high frequency QPOs in this work which for stellar mass black holes \sim hundreds of Hz while for supermassive black holes the QPO frequencies \sim mHz [40–43, 58, 59]. This can be understood in the following way. The deviation of the g_{tt} component of the metric from the Minkowski spacetime corresponds to the Newtonian potential. In our case, if we consider the spherically symmetric metric given by Eq. (5) the Newtonian potential is given by,

$$\Phi = \frac{G\tilde{M}}{r} e^{-k/r} \quad (21)$$

The force per unit mass can thus be evaluated,

$$F = -\frac{d\Phi}{dr} = \frac{G\tilde{M}}{r^2} e^{-k/r} (1 - k/r) = \frac{v^2}{r} \quad (22)$$

Therefore the velocity is given by:

$$v \simeq \sqrt{\frac{G\tilde{M}}{r} \left(1 - \frac{k}{r}\right)} e^{-k/2r} \quad (23)$$

Taking $r \simeq 8r_g$ and $k \simeq 0.2$ we note that

$$v \simeq 0.988 * \sqrt{\frac{G\tilde{M}}{r}} 0.975 \quad (24)$$

The dynamical timescale associated to matter rotating around the black hole is therefore given by,

$$t_d = \frac{r}{v} \sim 1.025 \sqrt{\frac{r^3}{G\tilde{M}}} \quad (25)$$

which for a $10M_\odot$ black hole at $r \simeq 8r_g$ turns out to be $t_d \sim 1.11ms$. The corresponding frequency is therefore \sim hundreds of Hertz.

Theoretical models aimed to explain these QPOs are dependent on the epicyclic frequencies which are inversely proportional to the black hole mass which explains the reason for lower frequencies in supermassive BHs [42, 58, 59]. Apart from HFQPOs, low frequency QPOs (LFQPOs) are also observed in some sources. We denote the observed HFQPOs by ν_{u1} and ν_{u2} while the low frequency QPO is denoted by ν_L .

We note that RE J1034+396 galaxy exhibits only a single QPO in its power spectrum [42, 60–62]. From Table 1 we note that HFQPOs in the BH sources generally appear in the ratio of 3:2 and we will consider only those sources in Table 1 (namely, the first five sources) which exhibit the 3:2 ratio HFQPOs. Therefore the data related to RE J1034+396 galaxy will not be used for subsequent analysis.

Source	Mass (M_{BH} in M_{\odot})	$\nu_{u1} \pm \Delta\nu_{u1}$ (in Hz)	$\nu_{u2} \pm \Delta\nu_{u2}$ (in Hz)	$\nu_L \pm \Delta\nu_L$ (in Hz)
GRO J1655 – 40	5.4 ± 0.3 [63]	441 ± 2 [64]	298 ± 4 [64]	17.3 ± 0.1 [64]
XTE J1550 – 564	9.1 ± 0.61 [65]	276 ± 3	184 ± 5	–
GRS 1915 + 105	$12.4^{+2.0}_{-1.8}$ [66]	168 ± 3	113 ± 5	–
H 1743 + 322	$8.0 - 14.07$ [67–69]	242 ± 3	166 ± 5	–
Sgr A*	$(3.5 - 4.9) \times 10^6$ [70, 71]	$(1.445 \pm 0.16) \times 10^{-3}$ [58, 72]	$(0.886 \pm 0.04) \times 10^{-3}$ [58, 72]	–
REJ1034 + 396	$(1 - 4) \times 10^6$ [42, 73–75]	$(2.5 - 2.8) \times 10^{-4}$ [42, 60–62]	–	–

Table 1: Black hole sources where high frequency QPOs (HFQPOs) are observed

Model	ν_1	ν_2	ν_3
Relativistic Precession Model (kinematic) [43, 76, 77]	ν_{ϕ}	$\nu_{\phi} - \nu_r$	$\nu_{\phi} - \nu_{\theta}$
Tidal Disruption Model (kinematic) [78–80]	$\nu_{\phi} + \nu_r$	ν_{θ}	–
Parametric Resonance Model (resonance) [81–83]	ν_{θ}	ν_r	–
Forced Resonance Model 1 (resonance) [81]	ν_{θ}	$\nu_{\theta} - \nu_r$	–
Forced Resonance Model 2 (resonance) [81]	$\nu_{\theta} + \nu_r$	ν_{θ}	–
Keplerian Resonance Model 1 (resonance) [84]	ν_{ϕ}	ν_r	–
Keplerian Resonance Model 2 (resonance) [84]	ν_{ϕ}	$2\nu_r$	–
Keplerian Resonance Model 3 (resonance) [84]	$3\nu_r$	ν_{ϕ}	–
Warped Disk Oscillation Model (resonance)	$2\nu_{\phi} - \nu_r$	$2(\nu_{\phi} - \nu_r)$	–
Non – axisymmetric Disk Oscillation Model 1 (resonance)	ν_{θ}	$\nu_{\phi} - \nu_r$	–
Non – axisymmetric Disk Oscillation Model 2 (resonance) [85–87]	$2\nu_{\phi} - \nu_{\theta}$	$\nu_{\phi} - \nu_r$	–

Table 2: Theoretical models explaining the HFQPOs in black holes.

4 Theoretical Models explaining quasi-periodic oscillations in the black hole power spectrum

This section is dedicated in reviewing some of the existing theoretical models proposed to explain the observed HFQPOs in BHs [43, 76–93]. These models mainly aim to explain the commensurability of the QPO frequencies. Table 2 presents the mathematical expressions for the model dependent QPO frequencies where the upper and lower HFQPOs are denoted by ν_1 and ν_2 while the low frequency QPO is denoted by ν_3 . From the table it is evident that the theoretical QPO frequencies are linear combinations of the angular frequency, the radial and the vertical epicyclic frequencies respectively given by $\nu_{\phi} = \frac{\omega_{\phi}}{2\pi}$, $\nu_r = \frac{\omega_r}{2\pi}$ and $\nu_{\theta} = \frac{\omega_{\theta}}{2\pi}$. Since the theoretical QPO frequencies depend purely on the background metric and not on the complex accretion physics, QPOs can potentially extract more accurate information about the background spacetime compared to other available observations, e.g., the iron line or the continuum-fitting methods.

- **Parametric resonance model:** The 3:2 ratio of the observed twin-peak HFQPOs (with frequencies ν_{u1} and ν_{u2}) in BH and NS sources indicates that QPOs might be a consequence of resonance

between various oscillation modes in the accretion disk [81, 94, 95]. When we considered circular, equatorial motion of test particles and slight perturbations δr and $\delta\theta$ in the orbit we tacitly assumed that the perturbations obey the equations of simple harmonic motion such that

$$\delta\ddot{r} + \omega_r^2\delta r = 0 ; \quad \delta\ddot{\theta} + \omega_\theta^2\delta\theta = 0 . \quad (26)$$

with frequencies $\omega_r = 2\pi\nu_r$ and $\omega_\theta = 2\pi\nu_\theta$ respectively. This implies that the motion in the radial and the vertical direction are uncoupled which is applicable to both thin disks as well as to more general accretion flow models, e.g. accretion tori [81, 94]. The presence of dissipation and pressure effects necessitate including forcing terms in Eq. (26)

$$\delta\ddot{r} + \omega_r^2\delta r = \omega_r^2 F_r(\delta r, \delta\theta, \delta\dot{r}, \delta\dot{\theta}) ; \quad \delta\ddot{\theta} + \omega_\theta^2\delta\theta = \omega_\theta^2 F_\theta(\delta r, \delta\theta, \delta\dot{r}, \delta\dot{\theta}) . \quad (27)$$

which are in general some non-linear functions of their arguments. The forms of F_r and F_θ are determined by the accretion flow model [82, 96].

In the parametric resonance model it is assumed that the radial epicyclic motion triggers the vertical epicyclic motion since random fluctuations in thin disks are expected to have $\delta r \gg \delta\theta$ [81–83, 94, 97]. In this scenario Eq. (27) assume the form,

$$\delta\ddot{r} + \omega_r^2\delta r = 0 \quad \delta\ddot{\theta} + \omega_\theta^2\delta\theta = -\omega_\theta^2\delta r\delta\theta \quad (28)$$

such that $\delta r = B \cos(\omega_r t)$ (where B is a constant) and the equation for $\delta\theta$ assumes the form of the Mathieu equation [98] given by

$$\delta\ddot{\theta} + \omega_\theta^2(1 + B\delta r)\delta\theta = 0 \quad (29)$$

and is excited when [82, 83, 98]

$$\frac{\nu_r}{\nu_\theta} = \frac{2}{n} , \quad \text{where } n \in \text{ positive integers} \quad (30)$$

For rotating non-singular BHs $\nu_\theta > \nu_r$ [72] (where $\nu_\theta = \omega_\theta/2\pi$ and $\nu_r = \omega_r/2\pi$) and therefore $n = 3$ gives rise to the strongest resonance which naturally explains the observed 3 : 2 ratio of the HFQPOs. This result has been confirmed by analytical calculations and numerical simulations [82, 83, 96].

- **Forced Resonance Model:** Thin disks or nearly Keplerian disks are more likely to exhibit parametric resonance [81, 94, 95]. In a more realistic flow however, couplings between δr and $\delta\theta$ are expected in addition to parametric resonance, arising from pressure, viscous or magnetic stresses present in the accretion flow leading to non-zero forcing terms [97]. Numerical simulations confirm that pressure couplings often lead to a resonant forcing of vertical oscillations by radial oscillations [94, 99]. Since the physics of accretion that leads to such resonant couplings is not very clearly understood the forcing terms are given by some mathematical ansatz, e.g.,

$$\delta\ddot{\theta} + \omega_\theta^2\delta\theta = -\omega_\theta^2\delta r\delta\theta + \mathcal{F}_\theta(\delta\theta) \quad (31)$$

such that $\delta r = B\cos(\omega_r t)$ while \mathcal{F}_θ corresponds to the non-linear terms in $\delta\theta$. It can be shown that Eq. (31) has solutions of the form,

$$\frac{\nu_\theta}{\nu_r} = \frac{m}{n} \quad \text{where } m \text{ and } n \text{ are natural numbers} \quad (32)$$

The presence of non-linear couplings lead to forced resonances, e.g. $m : n = 3 : 1$ and $m : n = 2 : 1$, apart from the $3 : 2$ parametric resonance which permits resonance between combinations of frequencies, e.g. $\nu_\theta - \nu_r$, $\nu_\theta + \nu_r$. The forced resonance model comprises of $3 : 1$ and $2 : 1$ forced resonances. In $3 : 1$ forced resonance model (denoted by Forced Resonance Model 1 or FRM1), the lower HFQPO is given by $\nu_2 = f_- = \nu_\theta - \nu_r$ while the upper HFQPO is given by $\nu_1 = \nu_\theta$. For $2 : 1$ forced resonance model the upper and lower high frequency QPOs are denoted by $\nu_1 = f_+ = \nu_\theta + \nu_r$ while $\nu_2 = \nu_\theta$ respectively.

- Keplerian resonance model:** In Keplerian resonance model one considers resonance between the orbital motion and the radial epicyclic motion [84, 94, 97, 100]. Keplerian resonance might arise under two possible circumstances: (a) trapping of non-axisymmetric g-mode oscillations induced by a corotation resonance in the inner region of relativistic thin accretion disks [100] and (b) when a pair of spatially separated coherent vortices with opposite vorticities oscillating with radial epicyclic frequencies couple with the spatially varying orbital angular frequencies [97, 101]. However, it was realized that g-mode oscillations are dampened by corotation resonance [102, 103] such that models invoking Keplerian resonance may not be very useful in explaining the HFQPOs in microquasars. Keplerian model consists of resonance between (i) $\nu_1 = \nu_\phi$ and $\nu_2 = \nu_r$ (which we denote as Keplerian Resonance Model 1 or KRM1), (ii) $\nu_1 = \nu_\phi$ and $\nu_2 = 2\nu_r$ (which we denote as Keplerian Resonance Model 2 or KRM2) and (iii) $\nu_1 = 3\nu_r$ and $\nu_2 = \nu_\phi$ (which we denote as Keplerian Resonance Model 3 or KRM3).
- Warped disk oscillation model:** This model which assumes a somewhat unusual disk geometry [86, 104] explains the HFQPOs in terms of non-linear resonances between the relativistic disk deformed by a warp with various disk oscillation modes [105–109]. Such resonances comprise of horizontal resonances inducing g-mode and p-mode oscillations as well as vertical resonances which can induce only the g-mode oscillations [106]. The origin of such resonances can be attributed to the non-monotonic variation of the radial epicyclic frequency with the radial distance r [106]. According to this model the upper high frequency QPO is given by $\nu_1 = 2\nu_\phi - \nu_r$ while the lower HFQPO is given by $\nu_2 = 2(\nu_\phi - \nu_r)$.
- Non-axisymmetric disk oscillation model:** Non-axisymmetric Disk-Oscillation models consider various combinations of non-axisymmetric disc oscillation modes as the origin of the HFQPOs [86, 87, 110–112]. These models which are variants of the Relativistic Precession model [86] include non-geodesic effects in the accretion flow by modelling the flow in terms of a slightly non-slender pressure-supported perfect fluid torus [87, 113, 114]. Two variants of non-axisymmetric disk-oscillation models are proposed in the literature: (i) the first (denoted by NADO1) [110–112]) assumes resonance between the vertical epicyclic frequency ($\nu_1 = \nu_\theta$) with $m = -1$ non-axisymmetric radial epicyclic frequency ($\nu_2 = \nu_\phi - \nu_r$) while the second (denoted by NADO2) considers resonance between the $m = -1$ non-axisymmetric radial epicyclic frequency ($\nu_2 = \nu_\phi - \nu_r$) with the $m = -2$ non-axisymmetric vertical epicyclic frequency ($\nu_1 = 2\nu_\phi - \nu_\theta$) [85–87] where m refers to the azimuthal wave number of the non-axisymmetric perturbation. However, the physical mechanisms inducing couplings between an axisymmetric and a non-axisymmetric mode or between the pairs non-axisymmetric modes are yet not very well-understood [86, 115].
- Relativistic precession model:** Models discussed so far are examples of resonance models. Relativistic precession model [43, 76] is a kinematic model which considers local motion of plasma in the accretion disk as the origin of QPOs. This model was initially proposed to address the HFQPOs in

neutron star sources and then subsequently extended for black holes [77]. In this model the upper and lower high frequency QPOs are associated with the orbital angular frequency ν_ϕ and the periastron precession frequency $\nu_\phi - \nu_r$. This model also addresses the observed low frequency QPO in black holes in terms of the nodal precession frequency $\nu_\phi - \nu_\theta$.

- **Tidal disruption model:** Another example of a kinematic model is the Tidal Disruption Model [78–80] which aims to explain the observed HFQPOs in terms of plasma orbiting the central object which may get tidally stretched forming ring-like features along the orbit giving rise to the modulation in the observed flux in the black hole power spectrum. According to this model $\nu_1 = \nu_\phi + \nu_r$ and $\nu_2 = \nu_\phi$.

We note from the above discussion that the theoretical QPO frequencies depend on the metric parameters a , k , the black hole mass \tilde{M} and the radius at which the QPO frequencies are generated r_{em} . Therefore we can directly constrain k and not q from the observations. Once we know k we can calculate q by using the previously determined masses. This is an artifact of the dependence of the Lagrangian density on mass. In this work k is denoted to be the non-linear electrodynamics (NED) charge parameter.

The QPO models we have considered here assume that the resonances involved in giving rise to the QPOs in the power spectrum are generated at the same circular orbit given by r_{em} [87, 104, 116]. This assumption holds true for the kinematic and the resonant models which we have discussed above. Apart from these there also exist certain diskoseismic models which are based on the assumption that the oscillatory modes giving rise to the HFQPOs are emitted at different radii of the accretion disk [88–90]. Magneto-hydrodynamic simulations [117–119] reveal that such models cannot explain the 3:2 HFQPOs adequately and therefore those models are not considered in this work. Further, we do not aim to extract the mass of the black hole sources from the observed QPO frequencies but rather use the previously estimated masses obtained from other independent observations, e.g., optical/NIR photometry (see Table 1).

5 Estimating the magnetic monopole charge from the observed QPOs

In this section we aim to derive the most favored value of k from observations related to QPOs. In order to accomplish this we compare the observed QPO frequencies given in Table 1 with the model dependent QPO frequencies in Table 2 and calculate the joint- χ^2 which is given by,

$$\chi^2(k) = \sum_{j=1}^5 \frac{\{\nu_{u1,j} - \nu_1(k, a_{\min}, \tilde{M}_{\min}, r_{em,\min})\}^2}{\sigma_{\nu_{u1},j}^2} + \sum_{j=1}^5 \frac{\{\nu_{u2,j} - \nu_2(k, a_{\min}, \tilde{M}_{\min}, r_{em,\min})\}^2}{\sigma_{\nu_{u2},j}^2}, \quad (33)$$

where ν_1 and ν_2 are the model dependent QPO frequencies, ν_{u1} and ν_{u2} are the observed QPO frequencies with errors given by $\sigma_{\nu_{u1}}^2$ and $\sigma_{\nu_{u2}}^2$ respectively. From Table 2 it is clear that the theoretical QPO frequencies depend on the orbital frequency and the epicyclic frequencies which are functions of the metric parameters k , a , \tilde{M} and the emission radius r_{em} . Since our goal is to determine the most favored value of k we do not minimize the joint- χ^2 with respect to all the four parameters. Instead we divide them into two categories [120] namely, (a) the “interesting parameters” (which is k) and (b) the “uninteresting parameters” (here a , \tilde{M} and r_{em}), derived from χ^2 minimization for various choices of the “interesting parameters”. We note that we do not estimate the black hole mass from the present analysis but use masses of these sources independently obtained from optical/NIR photometry (see Table 1).

To determine the most favored value of k we adopt the following procedure:

Comparison of mass estimates (in M_{\odot})	GRO J1655 – 40	XTE J1550 – 564	GRS 1915 + 105	H 1743 + 322	Sgr A*
Previous constraints	5.4 ± 0.3 [63]	9.1 ± 0.61 [65]	$12.4^{+2.0}_{-1.8}$ [66]	$8.0 - 14.07$ [67–69]	$(3.5 - 4.9) \times 10^{-3}$ [70, 71]
RPM	5.13 ($k \sim 0$)	9.3 ($k \sim 0$)	13.99 ($k \sim 0$)	12.06 ($k \sim 0$)	4.0×10^6 ($k \sim 0$)
TDM	7.0 ($k \sim 0.1$)	6.8 ($k \sim 0.1$)	8.6 ($k \sim 0.1$)	8.3 ($k \sim 0.1$)	4.4×10^6 ($k \sim 0.1$)
PRM	5.1 ($k \sim 0.1$)	8.49 ($k \sim 0.1$)	13.5 ($k \sim 0.1$)	10.98 ($k \sim 0.1$)	3.5×10^6 ($k \sim 0.1$)
FRM1	5.1 ($k \sim 0.4$)	9.61 ($k \sim 0.4$)	11.5 ($k \sim 0.4$)	9.37 ($k \sim 0.4$)	3.7×10^6 ($k \sim 0.4$)
FRM2	7.1 ($k \sim 0.3$)	7.29 ($k \sim 0.3$)	8.45 ($k \sim 0.3$)	7.75 ($k \sim 0.3$)	3.66×10^6 ($k \sim 0.3$)
KRM1	5.1($k \sim 0.1$)	8.49($k \sim 0.1$)	12.7($k \sim 0.1$)	8.1($k \sim 0.1$)	3.5×10^6 ($k \sim 0.1$)
KRM2	5.36 ($k \sim 0$)	8.94 ($k \sim 0$)	14.1 ($k \sim 0$)	13.08 ($k \sim 0$)	4.8×10^6 ($k \sim 0$)
KRM3	5.67 ($k \sim 0$)	9.65 ($k \sim 0$)	12.71 ($k \sim 0$)	10.33 ($k \sim 0$)	4.2×10^6 ($k \sim 0$)
WDOM	5.62 ($k \sim 0.2$)	9.45 ($k \sim 0.2$)	11.89 ($k \sim 0.2$)	11.43 ($k \sim 0.2$)	3.5×10^6 ($k \sim 0.2$)
NADO1	5.54 ($k \sim 0.4$)	9.42 ($k \sim 0.4$)	11.99 ($k \sim 0.4$)	9.55 ($k \sim 0.4$)	3.5×10^6 ($k \sim 0.4$)
NADO2	5.12 ($k \sim 0.3$)	9.14 ($k \sim 0.3$)	13.39 ($k \sim 0.3$)	12.26 ($k \sim 0.3$)	4.9×10^6 ($k \sim 0.3$)

Table 3: The above table presents the mass estimates of the BH sources considered in Table 1 from χ^2 minimization. The previously estimated masses are also reported.

1. We choose a given QPO model as mentioned in Table 2.
2. We next choose a source from Table 1.
3. Then we select a value of k which automatically fixes the allowed values of spin such that the central singularity is covered by a horizon. We vary the spin in this allowed range.
4. For the chosen k and spin we vary the black hole mass between $(M_{BH} - \Delta M_{BH}) \leq M_{BH} \leq (M_{BH} + \Delta M_{BH})$ where ΔM_{BH} is the error in the mass measurement (given in Table 1).
5. Further, for a given combination of k , a and M_{BH} we vary $r_{ms}(k, a) \leq r_{em} \leq r_{ms}(k, a) + 20r_g$.

Comparison of spin estimates	GRO J1655 – 40	XTE J1550 – 564	GRS 1915 + 105	H 1743 + 322	Sgr A*
Previous constraints	$a \sim 0.65-0.75$ [121] $a \sim 0.94-0.98$ [126] $a = 0.29 \pm 0.003$ [64]	$-0.11 < a < 0.71$ [122] $a = 0.55^{+0.15}_{-0.22}$ [122]	$a \sim 0.98$ [123] $a \sim 0.7$ [127] $a \sim 0.6 - 0.98$ [129] $a \sim 0.4 - 0.98$ [131]	$a = 0.2 \pm 0.3$ [124]	$a \sim 0.9$ [125] $a \sim 0.5$ [128] $a = 0.9959 \pm 0.0005$ [130] $a \lesssim 0.1$ [132]
RPM	0.3 ($k \sim 0$)	0.4 ($k \sim 0$)	0.3 ($k \sim 0$)	0.5 ($k \sim 0$)	0.97 ($k \sim 0$)
TDM	0.1 ($k \sim 0.1$)	0.2 ($k \sim 0.1$)	-0.3 ($k \sim 0.1$)	-0.3 ($k \sim 0.1$)	0.9 ($k \sim 0.1$)
PRM	0.8 ($k \sim 0.1$)	0.8 ($k \sim 0.1$)	0.8 ($k \sim 0.1$)	0.89 ($k \sim 0.1$)	0.9 ($k \sim 0.1$)
FRM1	-0.1 ($k \sim 0.4$)	0.1 ($k \sim 0.4$)	-0.3 ($k \sim 0.4$)	-0.1 ($k \sim 0.4$)	0.58 ($k \sim 0.4$)
FRM2	-0.1 ($k \sim 0.3$)	-0.1 ($k \sim 0.3$)	-0.4 ($k \sim 0.3$)	-0.3 ($k \sim 0.3$)	0.695 ($k \sim 0.3$)
KRM1	0.8997 ($k \sim 0.1$)	0.8997 ($k \sim 0.1$)	0.899 ($k \sim 0.1$)	0.89 ($k \sim 0.1$)	0.8997 ($k \sim 0.1$)
KRM2	0.32 ($k \sim 0$)	0.36 ($k \sim 0$)	0.32 ($k \sim 0$)	0.6 ($k \sim 0$)	0.97 ($k \sim 0$)
KRM3	0.22 ($k \sim 0$)	0.3 ($k \sim 0$)	0 ($k \sim 0$)	0.22 ($k \sim 0$)	0.99 ($k \sim 0$)
WDOM	0.0 ($k \sim 0.2$)	0.1 ($k \sim 0.2$)	-0.3 ($k \sim 0.2$)	0.1 ($k \sim 0.2$)	0.79 ($k \sim 0.2$)
NADO1	0.0 ($k \sim 0.4$)	0.1 ($k \sim 0.4$)	-0.3 ($k \sim 0.4$)	-0.1 ($k \sim 0.4$)	0.585 ($k \sim 0.4$)
NADO2	0.0 ($k \sim 0.3$)	0.1 ($k \sim 0.3$)	0.0 ($k \sim 0.3$)	0.2 ($k \sim 0.3$)	0.6 ($k \sim 0.3$)

Table 4: The above table presents the spin estimates of the BH sources considered in Table 1 from χ^2 minimization. The spin measurements obtained from earlier estimates are also reported.

6. The value of M_{BH} , a and r_{em} that minimizes the chi-square for the given k are denoted by M_m , a_m and r_m for the chosen source.
7. We repeat steps 3-6 for the other sources keeping k fixed.
8. Then we repeat steps 3-7 for the remaining values of k keeping the QPO model fixed. This enables us to calculate the magnitude of the joint- χ^2 for the chosen QPO model which we plot as a function of k . The magnitude of k where the joint- χ^2 minimizes is denoted by k_{min} and the value of the minimum χ^2 is denoted by χ^2_{min} . The M_m and a_m for each source corresponding to k_{min} are denoted by M_{min} and a_{min} and are reported in Table 3 and Table 4 respectively.
9. Models like RPM can also explain the low-frequency QPO observed in GRO J1655-40, when the

form of χ^2 is given by,

$$\chi^2(k) = \sum_j \frac{\{\nu_{u1,j} - \nu_1(k, a_{\min}, M_{\min}, r_{\text{em},\min})\}^2}{\sigma_{\nu_{u1},j}^2} + \sum_j \frac{\{\nu_{u2,j} - \nu_2(k, a_{\min}, M_{\min}, r_{\text{em},\min})\}^2}{\sigma_{\nu_{u2},j}^2} + \frac{\{\nu_{L,\text{GRO}} - \nu_3(k, a_{\min}, M_{\min}, r_{\text{em},\min})\}^2}{\sigma_{\nu_L,\text{GRO}}^2}. \quad (34)$$

10. We next choose another model from [Table 2](#) and repeat steps 2-9. This gives us the variation of χ^2 with k for each of the QPO models.
11. When the number of interesting parameters is one, the confidence intervals (i.e., $\Delta\chi^2$ from χ_{\min}^2) associated with 68%, 90% and 99% confidence levels are equal to 1, 2.71 and 6.63 [120]. The variation of χ^2 with k for each of the QPO models is illustrated in [Fig. 1](#) and [Fig. 2](#). It is important to note that in the present analysis we have assumed all the black holes to possess similar NED charge parameter k . Therefore, when we consider k as the interesting parameter we mean this to be the average charge associated with the black holes. This assumption is relevant as long as k varies in a very small range which in the present case is $0 \lesssim k \lesssim 0.7$ such that taking an average is meaningful. Moreover since $k \geq 0$, if $k = 0$ is favored observationally, it implies that the black holes in the sample possess no NED charge. Since we are observationally constraining the squared charge to mass ratio κ/r_g we do not face difficulties in considering black holes with largely different masses, i.e. if mass increases the charge increases proportionally such that the magnitude of k remains similar and in the range $0 \lesssim k \lesssim 0.7$ for the black holes in the sample. This allows us to consider a data sample comprising of four stellar mass and one supermassive black hole in this work.

This method is quite general and is not restricted to only regular black holes. The analysis works perfectly fine for regular black holes as well as for black holes with $r = 0$ curvature singularity as long as the metric is characterized by three parameters, namely, mass, spin and some charge. We have used this method to constrain the tidal charge parameter of braneworld black holes [133] and the magnetic monopole charge parameter of Bardeen black holes where Bardeen black holes are regular black holes with a de Sitter core [134]. This analysis can be further extended to more general regular black holes. In each case we estimate the dimensionless charge parameter (which is the charge scaled with the black hole mass) from the observations.

Therefore, method of analysis would not differ if we consider regular black holes with de Sitter cores. The assumption of Minkowski core comes in the choice of the mass function. For Bardeen black holes or braneworld black holes the mass functions are different. Each time the mass function is characterized by some charge parameter which has some physical interpretation. An external observer perceives the black hole through the spacetime curvature created by the metric parameters, namely, mass, spin and the charge, on which the epicyclic frequencies depend. If the metric comprises of more than three parameters then depending on the situation at hand the χ^2 can be characterized by more than one interesting parameters [120] in which case we will be required to generate contour plots of χ^2 to estimate the observationally favored magnitude of the charges which quantify the departure from GR.

Although we do not extract the black hole mass from the present analysis we provide independent estimates of spin since previous estimates of spin are derived using general relativity and different methods of spin measurements assuming general relativity yield largely disparate results (e.g., GRO J1655-40 [64]).

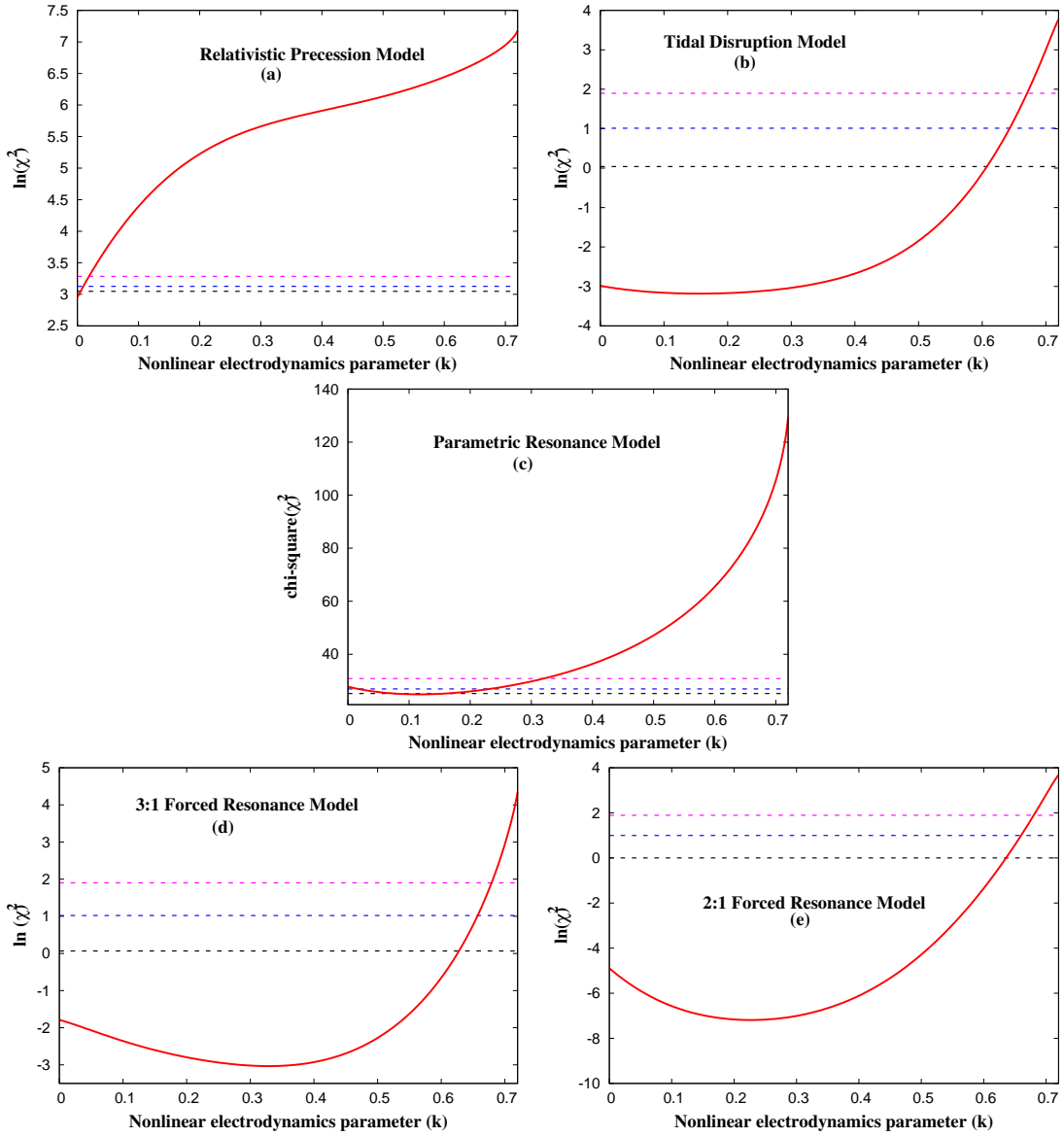


Figure 1: The above figure demonstrates the variation of χ^2 with the non-linear electrodynamic charge parameter k assuming the following QPO models: (a) Relativistic Precession Model (RPM), (b) Tidal Disruption Model (TDM), (c) Parametric Resonance Model (PRM), (d) 3:1 Forced Resonance Model (FRM1) and (e) 2:1 Forced Resonance Model (FRM2). The black, blue and magenta lines denote respectively the 68%, 90% and 99.7% confidence intervals corresponding to $\Delta\chi^2 = 1$, $\Delta\chi^2 = 2.71$ and $\Delta\chi^2 = 6.63$ from χ_{min}^2 .

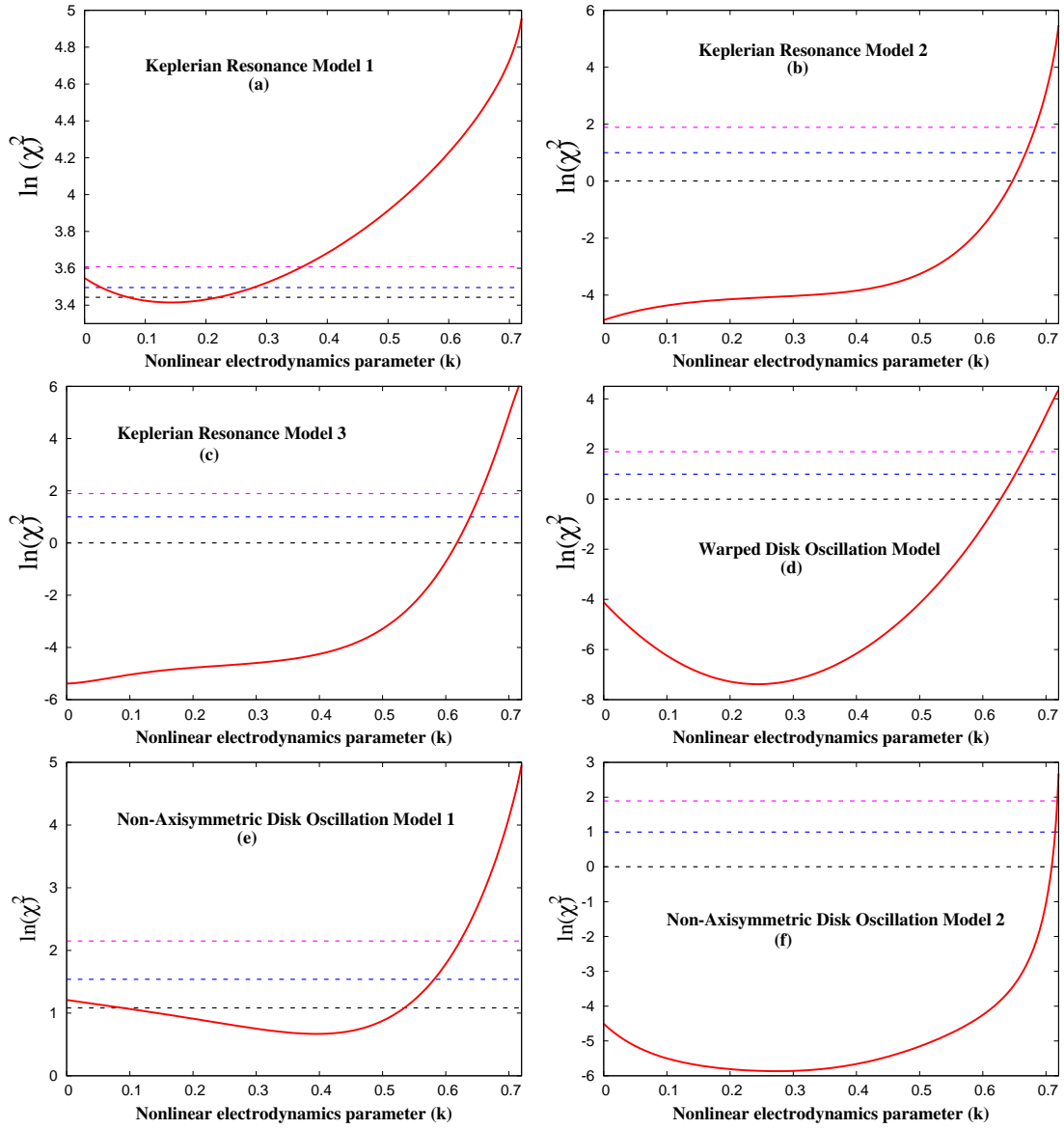


Figure 2: The above figure demonstrates the variation of χ^2 with the non-linear electrodynamic charge parameter k assuming the following models: (a) Keplerian Resonance Model 1, (b) Keplerian Resonance Model 2, (c) Keplerian Resonance Model 3, (d) Warped Disk Oscillation Model, (e) Non-axisymmetric Disc Oscillation Model 1 and (f) Non-axisymmetric Disc Oscillation Model. The black, blue and magenta lines denote respectively the 68%, 90% and 99.7% confidence intervals corresponding to $\Delta\chi^2 = 1$, $\Delta\chi^2 = 2.71$ and $\Delta\chi^2 = 6.63$ from χ^2_{min} .

In this regard we mention that earlier estimates of spin for GRS 1915+105, GRO J1655-40 and Sgr A* give rise to results with large discrepancies, e.g for GRS 1915+105, the Fe-line method gives $a \sim 0.6 - 0.98$ [129] while from Continuum Fitting Method the spin turns out to be intermediate ($a \sim 0.7$ [127]) as well as maximal ($a \sim 0.98$ [123]). With revised mass and inclination the spin of GRS 1915+105 turns out to be $0.4 < a < 0.98$. From Table 4 we note that our results based on PRM and KRM1 are consistent with previous measurements [123, 129, 131]. Spin measurements of the source XTE J1550-564 gives $-0.11 < a < 0.71$ from the Continuum Fitting method while Fe-line method yields a more stringent constraint $a = 0.55^{+0.15}_{-0.22}$ [122]. Our findings reveal that apart from PRM and KRM1 all the models yield spin in the range predicted by the Continuum Fitting method. Based on the Fe-line method and the Continuum-Fitting method the spin of GRO J1655-40 turns out to be $0.94 < a < 0.98$ [126] and $0.65 < a < 0.75$ [121] respectively while from QPO data assuming RPM the spin of the source is $a = 0.290 \pm 0.003$ [64]. From our analysis we find that our spin estimates based on RPM is in agreement with earlier spin measurements based on QPO related observations. Using Continuum-Fitting method [124] the spin of H1743-322 turns out to be $a = 0.2 \pm 0.3$ (with 68% confidence) and $a < 0.92$ (with 99.7% confidence). From Table 4 we note that models like RPM, FRM1, KRM3, WDOM, NADO1 and NADO2 yield results in agreement with previous findings. For the source Sgr A* the spin is obtained from its radio spectrum as well as motion of S2 stars. Since the radio spectrum of Sgr A* is difficult to model [125, 128, 135] diverse values of spin are obtained, e.g., $a \sim 0.9$ [125], $a \sim 0.5$ [128]. Investigating the motion of S2 stars near Sgr A* reveal the source has a spin $a \lesssim 0.1$ [132]. From the study of X-ray light curve of Sgr A* one finds that the object has a maximal spin with ($a = 0.9959 \pm 0.0005$) [130]. From our analysis we find that models like RPM, KRM3, WDOM and NADO1 yield a maximal spin as obtained in [130].

In Fig. 1 and Fig. 2 we plot χ^2 as a function of k for the QPO models discussed in Section 4. In particular, Fig. 1 depicts the variation of χ^2 with k for (a) Relativistic Precession Model (RPM), (b) Tidal Disruption Model (TDM), (c) Parametric Resonance Model (PRM), (d) 3:1 Forced Resonance Model (FRM1) and (e) 2:1 Forced Resonance Model (FRM2) while Fig. 2 illustrates the variation of χ^2 with k for (a) Keplerian Resonance Model 1 (KRM1) (b) Keplerian Resonance Model 2 (KRM2) (c) Keplerian Resonance Model 3 (KRM3) (d) Warped Disk Oscillation Model (WDOM) (e) Non-axisymmetric Disk Oscillation Model 1 (NADO1) and (f) Non-axisymmetric Disk Oscillation Model 2 (NADO2). The value of k where minimum χ^2 is attained represents the one most favored by observations. We denote this value of k by k_{min} . We also plot the confidence intervals, namely, with one interesting parameter, the $1 - \sigma$ confidence interval corresponds to $\chi^2 = \chi^2_{min} + 1$ (plotted with black dashed line), $2 - \sigma$ confidence interval corresponds to $\chi^2 = \chi^2_{min} + 2.71$ (plotted with blue dashed line) while the $3 - \sigma$ confidence interval corresponds to $\chi^2 = \chi^2_{min} + 6.63$ (plotted with magenta dashed line).

From Fig. 1 and Fig. 2 we note that models like Relativistic Precession Model (RPM), Parametric Resonance Model (PRM) and Keplerian Resonance Model 1 (KRM1) establish stringent constraints on k . According to RPM, χ^2 attains its minimum value when $k \simeq 0$ and discards $k \gtrsim 0.03$ outside $3 - \sigma$ confidence interval, for PRM χ^2_{min} is attained at $k \simeq 0.15$ and eliminates $k = 0$ outside $2 - \sigma$ confidence interval but includes general relativity within $3 - \sigma$. In particular PRM eliminates $k \gtrsim 0.3$ outside $3 - \sigma$ confidence interval. For KRM1, $k \simeq 0.15$ corresponds to χ^2_{min} while $k \gtrsim 0.35$ is eliminated outside $3 - \sigma$ confidence interval. This is interesting because PRM and RPM which discard large values of the charge parameter k are the most widely used QPO models. In particular, the commensurability of QPO frequencies can be most naturally explained by resonance models like PRM. While KRM1 also puts strong bounds on k , it is difficult to realize the resonant couplings assumed in KRM1 in the accretion scenario.

The remaining QPO models do not establish such strong bounds on k . The minimum χ^2 for the remaining QPO models correspond to (i) $k \simeq 0.2$ for the Tidal Disruption Model (TDM) (discards $k \gtrsim 0.65$ outside $3 - \sigma$ confidence interval), (ii) $k \simeq 0.35$ for the 3:1 Forced Resonance Model (discards $k \gtrsim 0.65$ outside

3- σ confidence interval), (iii) $k \simeq 0.25$ for the 2:1 Forced Resonance Model (discards $k \gtrsim 0.65$ outside 3- σ confidence interval), (iv) $k \simeq 0$ for the Keplerian Resonance Model 2 (discards $k \gtrsim 0.65$ outside 3- σ confidence interval), (v) $k \simeq 0$ for the Keplerian Resonance 3 (discards $k \gtrsim 0.6$ outside 3- σ confidence interval), (vi) $k \simeq 0.25$ for the Warped Disk Oscillation Model (discards $k \gtrsim 0.65$ outside 3- σ confidence interval), (vii) $k \simeq 0.45$ for the Non-axisymmetric Disk Oscillation Model 1 (discards $k \gtrsim 0.6$ outside 3- σ confidence interval) and (viii) $k \simeq 0.25$ for Non-axisymmetric Disk Oscillation Model 2. The above discussion reveals that all the QPO related observations generically discard large values of the charge parameter k .

6 Concluding Remarks

In this work we study regular black holes with an asymptotically Minkowski core which arise in gravity coupled to non-linear electrodynamics. Such black holes are associated with a non-linear electrodynamics (NED) charge parameter. Study of regular black holes is important as these can evade the curvature singularity at $r = 0$, an otherwise unavoidable feature in general relativity. Moreover, the exponential convergence factor arising in the mass function makes the quantum gravity model finite to all orders upto the Planck scale. Here we aim to decipher the signatures of the NED charge parameter from the observed quasi-periodic oscillations in black holes. Theoretical models aimed to address these peaks in the black hole power spectrum explain them in terms of local or collective motion of plasma near the marginally stable circular orbit. Thus, QPOs turn out to be a cleaner probe to the background spacetime compared to the continuum spectrum or the Fe-line which also depend on the complex physics of the accretion flow.

We review the various kinematic and resonant models of QPO proposed in the literature and compare the model based QPO frequencies with the available observations. In particular, we evaluate error estimator like the χ^2 which enables us to derive the observationally favored charge parameter and the spin corresponding to each of the black holes. Our analysis reveal that most QPO models favor the general relativistic scenario or small values of k . Particularly, models like RPM, PRM and KRM1 establish stringent constraints on the NED charge parameter, e.g, PRM and KRM1 favor small but non-trivial values of the charge parameter, viz, $k \simeq 0.15$ but eliminates large values of k e.g. $k \gtrsim 0.35$ outside 3- σ confidence interval. The Relativistic Precession model on the other hand favor $k = 0$ and discard $k \gtrsim 0.03$ outside 99.7% confidence level. This is interesting because the most extensively used QPO models like RPM and PRM impose very strong bounds on the NED charge parameter. We further note that all the QPO models studied here discard large values of the charge parameter. It is important to note that the observationally preferred magnitude of k corresponds to the average charge of the black holes and in the present analysis we assume that the black holes considered here have similar charges. A separate analysis considering black holes with different charges can be done in which case the number of interesting parameters will be two i.e., charge and spin and one needs to consider the sources individually to obtain constraints on the observationally favored magnitude of these two parameters. We leave this analysis for a future work.

Although it might seem from the present analysis that large values of the non-linear electrodynamics charge parameter are disfavored by observations related to QPOs, these results have certain limitations. First, our findings are purely model dependent, i.e., despite observing QPOs for decades there is no common consensus on the correct choice of the QPO model. While some believe that HFQPOs in black holes should be explained by a single QPO model which is yet to be determined, others believe that the correct choice of the QPO model may be source dependent. Second, there are very few black holes which exhibit HFQPOs in their power spectrum, and hence our results are limited due to poor statistics. Moreover, the present data has large errors, which further limits our analysis. This can however be overcome with the launch

of the ESA (European Space Agency) X-ray mission LOFT (Large Observatory for X-ray Timing) which aims to improve the precision of data by an order of magnitude. However, with the available data sample, precision and models, the present analysis provides a possible framework which may be used to constrain several alternatives to general relativity, with QPO related observations.

Acknowledgement

Research of I.B. is funded by the Start-Up Research Grant from SERB, DST, Government of India (Reg. No. SRG/2021/000418).

References

- [1] S. W. Hawking and G. F. R. Ellis, *The Large Scale Structure of Space-Time*. Cambridge Monographs on Mathematical Physics. Cambridge University Press, 2, 2011.
- [2] P. Horava and E. Witten, “Heterotic and type I string dynamics from eleven-dimensions,” *Nucl. Phys. B* **460** (1996) 506–524, [arXiv:hep-th/9510209 \[hep-th\]](#). [[397\(1995\)](#)].
- [3] P. Horava and E. Witten, “Eleven-dimensional supergravity on a manifold with boundary,” *Nucl. Phys. B* **475** (1996) 94–114, [arXiv:hep-th/9603142 \[hep-th\]](#).
- [4] J. Polchinski, “String theory. Vol. 1: An introduction to the bosonic string,”.
- [5] J. Polchinski, “String theory. Vol. 2: Superstring theory and beyond,”.
- [6] A. Ashtekar, T. Pawłowski, and P. Singh, “Quantum nature of the big bang,” *Phys. Rev. Lett.* **96** (2006) 141301, [arXiv:gr-qc/0602086 \[gr-qc\]](#).
- [7] A. Ashtekar, T. Pawłowski, and P. Singh, “Quantum Nature of the Big Bang: An Analytical and Numerical Investigation. I.,” *Phys. Rev. D* **73** (2006) 124038, [arXiv:gr-qc/0604013](#).
- [8] A. Ashtekar, T. Pawłowski, and P. Singh, “Quantum Nature of the Big Bang: Improved dynamics,” *Phys. Rev. D* **74** (2006) 084003, [arXiv:gr-qc/0607039](#).
- [9] D. Kothawala, “Minimal Length and Small Scale Structure of Spacetime,” *Phys. Rev. D* **88** no. 10, (2013) 104029, [arXiv:1307.5618 \[gr-qc\]](#).
- [10] D. Kothawala, “Small scale structure of spacetime in presence of a minimal length,” *J. Phys. Conf. Ser.* **600** no. 1, (2015) 012069.
- [11] S. Ansoldi, “Spherical black holes with regular center: A Review of existing models including a recent realization with Gaussian sources,” in *Conference on Black Holes and Naked Singularities*. 2, 2008. [arXiv:0802.0330 \[gr-qc\]](#).
- [12] E. B. Gliner, “Algebraic Properties of the Energy-momentum Tensor and Vacuum-like States of Matter,” *Soviet Journal of Experimental and Theoretical Physics* **22** (Feb., 1966) 378.
- [13] Z.-Y. Fan and X. Wang, “Construction of Regular Black Holes in General Relativity,” *Phys. Rev. D* **94** no. 12, (2016) 124027, [arXiv:1610.02636 \[gr-qc\]](#).

- [14] V. P. Frolov, M. A. Markov, and V. F. Mukhanov, “Black Holes as Possible Sources of Closed and Semiclosed Worlds,” *Phys. Rev. D* **41** (1990) 383.
- [15] V. F. Mukhanov and R. H. Brandenberger, “A Nonsingular universe,” *Phys. Rev. Lett.* **68** (1992) 1969–1972.
- [16] R. H. Brandenberger, V. F. Mukhanov, and A. Sornborger, “A Cosmological theory without singularities,” *Phys. Rev. D* **48** (1993) 1629–1642, [arXiv:gr-qc/9303001](https://arxiv.org/abs/gr-qc/9303001).
- [17] B. Carter, “Global structure of the kerr family of gravitational fields,” *Phys. Rev.* **174** (Oct, 1968) 1559–1571. <https://link.aps.org/doi/10.1103/PhysRev.174.1559>.
- [18] E. Ayon-Beato and A. Garcia, “The Bardeen model as a nonlinear magnetic monopole,” *Phys. Lett. B* **493** (2000) 149–152, [arXiv:gr-qc/0009077](https://arxiv.org/abs/gr-qc/0009077).
- [19] E. Ayon-Beato and A. Garcia, “Regular black hole in general relativity coupled to nonlinear electrodynamics,” *Phys. Rev. Lett.* **80** (1998) 5056–5059, [arXiv:gr-qc/9911046](https://arxiv.org/abs/gr-qc/9911046).
- [20] E. Ayon-Beato and A. Garcia, “Four parametric regular black hole solution,” *Gen. Rel. Grav.* **37** (2005) 635, [arXiv:hep-th/0403229](https://arxiv.org/abs/hep-th/0403229).
- [21] K. A. Bronnikov, “Regular magnetic black holes and monopoles from nonlinear electrodynamics,” *Phys. Rev. D* **63** (2001) 044005, [arXiv:gr-qc/0006014](https://arxiv.org/abs/gr-qc/0006014).
- [22] A. Borde, “Regular black holes and topology change,” *Phys. Rev. D* **55** (1997) 7615–7617, [arXiv:gr-qc/9612057](https://arxiv.org/abs/gr-qc/9612057).
- [23] C. Barrabes and V. P. Frolov, “How many new worlds are inside a black hole?,” *Phys. Rev. D* **53** (1996) 3215–3223, [arXiv:hep-th/9511136](https://arxiv.org/abs/hep-th/9511136).
- [24] E. Ayon-Beato and A. Garcia, “Nonsingular charged black hole solution for nonlinear source,” *Gen. Rel. Grav.* **31** (1999) 629–633, [arXiv:gr-qc/9911084](https://arxiv.org/abs/gr-qc/9911084).
- [25] A. Bonanno and M. Reuter, “Renormalization group improved black hole space-times,” *Phys. Rev. D* **62** (2000) 043008, [arXiv:hep-th/0002196](https://arxiv.org/abs/hep-th/0002196).
- [26] P. Nicolini, A. Smailagic, and E. Spallucci, “Noncommutative geometry inspired Schwarzschild black hole,” *Phys. Lett. B* **632** (2006) 547–551, [arXiv:gr-qc/0510112](https://arxiv.org/abs/gr-qc/0510112).
- [27] Y. S. Myung, Y.-W. Kim, and Y.-J. Park, “Quantum Cooling Evaporation Process in Regular Black Holes,” *Phys. Lett. B* **656** (2007) 221–225, [arXiv:gr-qc/0702145](https://arxiv.org/abs/gr-qc/0702145).
- [28] S. A. Hayward, “Formation and evaporation of nonsingular black holes,” *Phys. Rev. Lett.* **96** (Jan, 2006) 031103. <https://link.aps.org/doi/10.1103/PhysRevLett.96.031103>.
- [29] H. Culetu, “On a regular charged black hole with a nonlinear electric source,” *Int. J. Theor. Phys.* **54** no. 8, (2015) 2855–2863, [arXiv:1408.3334](https://arxiv.org/abs/1408.3334) [gr-qc].
- [30] M. R. Brown, “Is Quantum Gravity Finite?,” in *Oxford Conference on Quantum Gravity*. 1980.

- [31] J. W. Moffat, “Quantum gravity resolution to the cosmological constant problem,” [arXiv:hep-ph/0102088](#).
- [32] E. T. Newman and A. I. Janis, “Note on the Kerr spinning particle metric,” *J. Math. Phys.* **6** (1965) 915–917.
- [33] M. Azreg-Aïnou, “Generating rotating regular black hole solutions without complexification,” *Phys. Rev. D* **90** no. 6, (2014) 064041, [arXiv:1405.2569 \[gr-qc\]](#).
- [34] M. Azreg-Aïnou, “From static to rotating to conformal static solutions: Rotating imperfect fluid wormholes with(out) electric or magnetic field,” *Eur. Phys. J. C* **74** no. 5, (2014) 2865, [arXiv:1401.4292 \[gr-qc\]](#).
- [35] M. Azreg-Aïnou, “Regular and conformal regular cores for static and rotating solutions,” *Phys. Lett. B* **730** (2014) 95–98, [arXiv:1401.0787 \[gr-qc\]](#).
- [36] L. Modesto and P. Nicolini, “Charged rotating noncommutative black holes,” *Phys. Rev. D* **82** (2010) 104035, [arXiv:1005.5605 \[gr-qc\]](#).
- [37] S. G. Ghosh, “A nonsingular rotating black hole,” *Eur. Phys. J. C* **75** no. 11, (2015) 532, [arXiv:1408.5668 \[gr-qc\]](#).
- [38] C. Bambi, “Probing the space-time geometry around black hole candidates with the resonance models for high-frequency QPOs and comparison with the continuum-fitting method,” *JCAP* **09** (2012) 014, [arXiv:1205.6348 \[gr-qc\]](#).
- [39] C. Bambi, “Testing the nature of the black hole candidate in GRO J1655-40 with the relativistic precession model,” *Eur. Phys. J. C* **75** no. 4, (2015) 162, [arXiv:1312.2228 \[gr-qc\]](#).
- [40] W. H. G. Lewin and M. van der Klis, *Compact Stellar X-ray Sources*, vol. 39. 2006.
- [41] M. van der Klis, “Millisecond oscillations in x-ray binaries,” *Ann. Rev. Astron. Astrophys.* **38** (2000) 717–760, [arXiv:astro-ph/0001167](#).
- [42] M. Gierliński, M. Middleton, M. Ward, and C. Done, “A periodicity of ~ 1 hour in X-ray emission from the active galaxy RE J1034+396,” *nat* **455** no. 7211, (Sept., 2008) 369–371.
- [43] L. Stella and M. Vietri, “khz quasiperiodic oscillations in low-mass x-ray binaries as probes of general relativity in the strong-field regime,” *Phys. Rev. Lett.* **82** (Jan, 1999) 17–20. <https://link.aps.org/doi/10.1103/PhysRevLett.82.17>.
- [44] R. Kumar and S. G. Ghosh, “Photon ring structure of rotating regular black holes and no-horizon spacetimes,” *Class. Quant. Grav.* **38** no. 8, (2021) 8, [arXiv:2004.07501 \[gr-qc\]](#).
- [45] I. H. Salazar, A. Garcia, and J. Plebanski, “Duality Rotations and Type D Solutions to Einstein Equations With Nonlinear Electromagnetic Sources,” *J. Math. Phys.* **28** (1987) 2171–2181.
- [46] K. A. Bronnikov, “Comment on “Construction of regular black holes in general relativity”,” *Phys. Rev. D* **96** no. 12, (2017) 128501, [arXiv:1712.04342 \[gr-qc\]](#).
- [47] B. Toshmatov, Z. Stuchlík, and B. Ahmedov, “Comment on “Construction of regular black holes in general relativity”,” *Phys. Rev. D* **98** no. 2, (2018) 028501, [arXiv:1807.09502 \[gr-qc\]](#).

- [48] A. Simpson and M. Visser, “Regular black holes with asymptotically Minkowski cores,” *Universe* **6** no. 1, (2019) 8, [arXiv:1911.01020 \[gr-qc\]](#).
- [49] H. Culetu, “On a regular modified Schwarzschild spacetime,” [arXiv:1305.5964 \[gr-qc\]](#).
- [50] S. R. Valluri, D. J. Jeffrey, and R. M. Corless, “Some applications of the Lambert W function to physics,” *Can. J. Phys.* **78** (2000) 823–831.
- [51] P. Boonserm and M. Visser, “Bounding the greybody factors for Schwarzschild black holes,” *Phys. Rev. D* **78** (2008) 101502, [arXiv:0806.2209 \[gr-qc\]](#).
- [52] P. Boonserm and M. Visser, “Quasi-normal frequencies: Key analytic results,” *JHEP* **03** (2011) 073, [arXiv:1005.4483 \[math-ph\]](#).
- [53] P. Boonserm, T. Ngampitipan, and M. Visser, “Regge-Wheeler equation, linear stability, and greybody factors for dirty black holes,” *Phys. Rev. D* **88** (2013) 041502, [arXiv:1305.1416 \[gr-qc\]](#).
- [54] P. Boonserm, T. Ngampitipan, A. Simpson, and M. Visser, “Exponential metric represents a traversable wormhole,” *Phys. Rev. D* **98** no. 8, (2018) 084048, [arXiv:1805.03781 \[gr-qc\]](#).
- [55] H. Sonoda, “Solving renormalization group equations with the Lambert W function,” *Phys. Rev. D* **87** no. 8, (2013) 085023, [arXiv:1302.6069 \[hep-th\]](#).
- [56] H. Sonoda, “Analytic form of the effective potential in the large N limit of a real scalar theory in four dimensions,” [arXiv:1302.6059 \[hep-th\]](#).
- [57] R. Kumar and S. G. Ghosh, “Black Hole Parameter Estimation from Its Shadow,” *Astrophys. J.* **892** (2020) 78, [arXiv:1811.01260 \[gr-qc\]](#).
- [58] G. Torok, “A Possible 3:2 orbital epicyclic resonance in QPOs frequencies of Sgr A*,” *Astron. Astrophys.* **440** (2005) 1, [arXiv:astro-ph/0412500](#).
- [59] B. Aschenbach, “Measuring mass and angular momentum of black holes with high-frequency quasiperiodic oscillations,” *Astron. Astrophys.* **425** (2004) 1075–1082, [arXiv:astro-ph/0406545](#).
- [60] M. Middleton, C. Done, M. Ward, M. Gierlinski, and N. Schurch, “RE J1034+396: The origin of the soft X-ray excess and QPO,” *Mon. Not. Roy. Astron. Soc.* **394** (2009) 250, [arXiv:0807.4847 \[astro-ph\]](#).
- [61] C. Jin, C. Done, and M. Ward, “Re-observing the NLS1 Galaxy RE J1034+396. I. the Long-term, Recurrent X-ray QPO with a High Significance,” *Mon. Not. Roy. Astron. Soc.* **495** (2020) 3538, [arXiv:2005.05857 \[astro-ph.HE\]](#).
- [62] C. Jin, C. Done, and M. Ward, “Re-observing the NLS1 galaxy RE J1034+396 – II. New insights on the soft X-ray excess, QPO, and the analogy with GRS 1915+105,” *Mon. Not. Roy. Astron. Soc.* **500** no. 2, (2020) 2475–2495, [arXiv:2007.14704 \[astro-ph.HE\]](#).
- [63] M. E. Beer and P. Podsiadlowski, “The quiescent light curve and evolutionary state of gro j1655-40,” *Mon. Not. Roy. Astron. Soc.* **331** (2002) 351, [arXiv:astro-ph/0109136](#).

- [64] S. E. Motta, T. M. Belloni, L. Stella, T. Muñoz Darias, and R. Fender, “Precise mass and spin measurements for a stellar-mass black hole through X-ray timing: the case of GRO J1655–40,” *Mon. Not. Roy. Astron. Soc.* **437** no. 3, (2014) 2554–2565, [arXiv:1309.3652 \[astro-ph.HE\]](#).
- [65] J. A. Orosz, J. F. Steiner, J. E. McClintock, M. A. P. Torres, R. A. Remillard, C. D. Bailyn, and J. M. Miller, “An Improved Dynamical Model for the Microquasar XTE J1550-564,” *Astrophys. J.* **730** (2011) 75, [arXiv:1101.2499 \[astro-ph.SR\]](#).
- [66] M. J. Reid, J. E. McClintock, J. F. Steiner, D. Steeghs, R. A. Remillard, V. Dhawan, and R. Narayan, “A Parallax Distance to the Microquasar GRS 1915+105 and a Revised Estimate of its Black Hole Mass,” *Astrophys. J.* **796** (2014) 2, [arXiv:1409.2453 \[astro-ph.GA\]](#).
- [67] G. Pei, S. Nampalliwar, C. Bambi, and M. J. Middleton, “Blandford-Znajek mechanism in black holes in alternative theories of gravity,” *Eur. Phys. J. C* **76** no. 10, (2016) 534, [arXiv:1606.04643 \[gr-qc\]](#).
- [68] A. Bhattacharjee, I. Banerjee, A. Banerjee, D. Debnath, and S. K. Chakrabarti, “The 2004 Outburst of BHC H1743-322: Analysis of spectral and timing properties using the TCAF Solution,” *Mon. Not. Roy. Astron. Soc.* **466** (2017) 1372–1381, [arXiv:1901.00810 \[astro-ph.HE\]](#).
- [69] J. Petri, “A new model for QPOs in accreting black holes: application to the microquasar GRS 1915+105,” *Astrophys. Space Sci.* **318** (2008) 181–186, [arXiv:0809.3115 \[astro-ph\]](#).
- [70] A. M. Ghez *et al.*, “Measuring Distance and Properties of the Milky Way’s Central Supermassive Black Hole with Stellar Orbits,” *Astrophys. J.* **689** (2008) 1044–1062, [arXiv:0808.2870 \[astro-ph\]](#).
- [71] S. Gillessen, F. Eisenhauer, S. Trippe, T. Alexander, R. Genzel, F. Martins, and T. Ott, “Monitoring stellar orbits around the Massive Black Hole in the Galactic Center,” *Astrophys. J.* **692** (2009) 1075–1109, [arXiv:0810.4674 \[astro-ph\]](#).
- [72] Z. Stuchlík and A. Kotrlová, “Orbital resonances in discs around braneworld Kerr black holes,” *Gen. Rel. Grav.* **41** (2009) 1305–1343, [arXiv:0812.5066 \[astro-ph\]](#).
- [73] C. Jin, M. Ward, C. Done, and J. Gelbord, “A combined optical and X-ray study of unobscured type 1 active galactic nuclei - I. Optical spectra and spectral energy distribution modelling,” *mnras* **420** no. 3, (Mar., 2012) 1825–1847, [arXiv:1109.2069 \[astro-ph.HE\]](#).
- [74] B. Czerny, B. You, A. Kurcz, J. Średzińska, K. Hryniewicz, M. Nikolajuk, M. Krupa, J. M. Wang, C. Hu, and P. T. Życki, “The mass of the black hole in RE J1034+396,” *Astron. Astrophys.* **594** (2016) A102, [arXiv:1601.02498 \[astro-ph.GA\]](#).
- [75] K. Chaudhury *et al.*, “Long-term X-ray variability characteristics of the narrow-line Seyfert 1 galaxy RE J1034+396,” *Mon. Not. Roy. Astron. Soc.* **478** no. 4, (2018) 4830–4836, [arXiv:1807.06460 \[astro-ph.HE\]](#).
- [76] L. Stella and M. Vietri, “Lense-Thirring precession and QPOS in low mass x-ray binaries,” *Astrophys. J. Lett.* **492** (1998) L59, [arXiv:astro-ph/9709085](#).

- [77] L. Stella, M. Vietri, and S. M. Morsink, “Correlations in the quasi-periodic oscillation frequencies of low-mass x-ray binaries and the relativistic precession model,” *The Astrophysical Journal* **524** no. 1, (Oct, 1999) L63–L66. <https://doi.org/10.1086/312291>.
- [78] A. Cadez, M. Calvani, and U. Kostic, “On the tidal evolution of the orbits of low-mass satellites around black holes,” *Astron. Astrophys.* **487** (2008) 527–532, [arXiv:0809.1783](https://arxiv.org/abs/0809.1783) [astro-ph].
- [79] U. Kostic, A. Cadez, M. Calvani, and A. Gomboc, “Tidal effects on small bodies by massive black holes,” *Astron. Astrophys.* **496** (2009) 307, [arXiv:0901.3447](https://arxiv.org/abs/0901.3447) [astro-ph.HE].
- [80] C. Germana, U. Kostic, A. Cadez, and M. Calvani, “Tidal disruption of small satellites orbiting black holes,” *AIP Conf. Proc.* **1126** no. 1, (2009) 367–369, [arXiv:0902.2134](https://arxiv.org/abs/0902.2134) [astro-ph.HE].
- [81] W. Kluzniak and M. A. Abramowicz, “Parametric epicyclic resonance in black hole disks: qpos in micro-quasars,” [arXiv:astro-ph/0203314](https://arxiv.org/abs/astro-ph/0203314).
- [82] M. A. Abramowicz, V. Karas, W. Kluzniak, W. H. Lee, and P. Rebusco, “Nonlinear resonance in nearly geodesic motion in low mass x-ray binaries,” *Publ. Astron. Soc. Jap.* **55** (2003) 466–467, [arXiv:astro-ph/0302183](https://arxiv.org/abs/astro-ph/0302183).
- [83] P. Rebusco, “Twin peaks kHz QPOs: Mathematics of the 3:2 orbital resonance,” *Publ. Astron. Soc. Jap.* **56** (2004) 553, [arXiv:astro-ph/0403341](https://arxiv.org/abs/astro-ph/0403341).
- [84] M. A. Nowak, R. V. Wagoner, M. C. Begelman, and D. E. Lehr, “The 67 hz feature in the black hole candidate grs 1915+105 as a possible “diskoseismic” mode,” *Astrophys. J. Lett.* **477** (1997) L91, [arXiv:astro-ph/9612142](https://arxiv.org/abs/astro-ph/9612142).
- [85] G. Torok, P. Bakala, E. Sramkova, Z. Stuchlik, and M. Urbanec, “On mass-constraints implied by the relativistic precession model of twin-peak quasi-periodic oscillations in Circinus X-1,” *Astrophys. J.* **714** (2010) 748–757, [arXiv:1008.0088](https://arxiv.org/abs/1008.0088) [astro-ph.HE].
- [86] G. Torok, A. Kotrlova, E. Sramkova, and Z. Stuchlik, “Confronting the models of 3:2 quasiperiodic oscillations with the rapid spin of the microquasar GRS 1915+105,” *Astron. Astrophys.* **531** (2011) A59, [arXiv:1103.2438](https://arxiv.org/abs/1103.2438) [astro-ph.HE].
- [87] A. Kotrlová, E. Šrámková, G. Török, K. Goluchová, J. Horák, O. Straub, D. Lancová, Z. Stuchlík, and M. A. Abramowicz, “Models of high-frequency quasi-periodic oscillations and black hole spin estimates in Galactic microquasars,” *Astron. Astrophys.* **643** (2020) A31, [arXiv:2008.12963](https://arxiv.org/abs/2008.12963) [astro-ph.HE].
- [88] S. Kato and J. Fukue, “Trapped Radial Oscillations of Gaseous Disks around a Black Hole,” *Publ. Astron. Soc. Jap.* **32** (1980) 377.
- [89] C. A. Perez, A. S. Silbergleit, R. V. Wagoner, and D. E. Lehr, “Relativistic diskoseismology. 1. Analytical results for ‘gravity modes’,” *Astrophys. J.* **476** (1997) 589–604, [arXiv:astro-ph/9601146](https://arxiv.org/abs/astro-ph/9601146).
- [90] A. S. Silbergleit, R. V. Wagoner, and M. Ortega-Rodriguez, “Relativistic diskoseismology. 2. Analytical results for C modes,” *Astrophys. J.* **548** (2001) 335–347, [arXiv:astro-ph/0004114](https://arxiv.org/abs/astro-ph/0004114).

- [91] J. Dexter and O. Blaes, “A model of the steep power law spectra and high-frequency quasi-periodic oscillations in luminous black hole X-ray binaries,” *Mon. Not. Roy. Astron. Soc.* **438** no. 4, (2014) 3352–3357, [arXiv:1312.0941 \[astro-ph.HE\]](#).
- [92] L. Rezzolla, S. Yoshida, and O. Zanotti, “Oscillations of vertically integrated relativistic tori - 1. Axisymmetric modes in a Schwarzschild space-time,” *Mon. Not. Roy. Astron. Soc.* **344** (2003) 978, [arXiv:astro-ph/0307488](#).
- [93] L. Rezzolla, S. Yoshida, T. J. Maccarone, and O. Zanotti, “A New simple model for high frequency quasi periodic oscillations in black hole candidates,” *Mon. Not. Roy. Astron. Soc.* **344** (2003) L37, [arXiv:astro-ph/0307487](#).
- [94] M. A. Abramowicz and W. Kluźniak, “A precise determination of black hole spin in GRO J1655-40,” *Astron. Astrophys.* **374** (2001) L19–L20, [arXiv:astro-ph/0105077 \[astro-ph\]](#).
- [95] W. Kluzniak and M. A. Abramowicz, “Strong-Field Gravity and Orbital Resonance in Black Holes and Neutron Stars — kHz Quasi-Periodic Oscillations (QPO),” *Acta Physica Polonica B* **32** no. 11, (Nov., 2001) 3605.
- [96] J. Horak, M. Abramowicz, V. Karas, and W. Kluzniak, “Of NBOs and kHz QPOs: A Low-frequency modulation in resonant oscillations of relativistic accretion disks,” *Publ. Astron. Soc. Jap.* **56** (2004) 819–822, [arXiv:astro-ph/0408090](#).
- [97] G. Török, M. A. Abramowicz, W. Kluźniak, and Z. Stuchlík, “The orbital resonance model for twin peak kHz quasi periodic oscillations in microquasars,” *Astron. Astrophys.* **436** no. 1, (2005) 1–8.
- [98] L. D. Landau and E. M. Lifshitz, *Mechanics*. 1969.
- [99] W. H. Lee, M. A. Abramowicz, and W. Kluźniak, “Resonance in Forced Oscillations of an Accretion Disk and Kilohertz Quasi-periodic Oscillations,” *apjl* **603** no. 2, (Mar., 2004) L93–L96, [arXiv:astro-ph/0402084 \[astro-ph\]](#).
- [100] S. Kato, “Trapping of Non-Axisymmetric g-Mode Oscillations in Thin Relativistic Disks and kHz QPOs,” *PASJ* **53** no. 5, (Oct., 2001) L37–L39.
- [101] M. A. Abramowicz, G. Björnsson, and J. E. Pringle, *Theory of Black Hole Accretion Discs*. 2010.
- [102] L.-X. Li, J. Goodman, and R. Narayan, “Non-axisymmetric g-mode and p-mode instability in a thin accretion disk,” *Astrophys. J.* **593** (2003) 980, [arXiv:astro-ph/0210455](#).
- [103] S. Kato, “Damping and Frequencies of Non-Axisymmetric Trapped g-Mode Oscillations,” *PASJ* **55** (Feb., 2003) 257–265.
- [104] K. Yagi and L. C. Stein, “Black Hole Based Tests of General Relativity,” *Class. Quant. Grav.* **33** no. 5, (2016) 054001, [arXiv:1602.02413 \[gr-qc\]](#).
- [105] S. Kato, “Basic Properties of Thin-Disk Oscillations ¹,” *pasj* **53** no. 1, (Feb., 2001) 1–24.
- [106] S. Kato, “Wave-Warp Resonant Interactions in Relativistic Disks and kHz QPOs,” *pasj* **56** (June, 2004) 559–567.

- [107] S. Kato, “Resonant Excitation of Disk Oscillations by Warps: A Model of kHz QPOs,” *pasj* **56** (Oct., 2004) 905–922, [arXiv:astro-ph/0409051](#) [astro-ph].
- [108] S. Kato, “A Vertical Resonance of g-Mode Oscillations in Warped Disks and QPOs in Low-Mass X-Ray Binaries,” *pasj* **57** (Aug., 2005) 699–703, [arXiv:astro-ph/0507234](#) [astro-ph].
- [109] S. Kato, “Resonant Excitation of Disk Oscillations in Deformed Disks II: A Model of High-Frequency QPOs,” *pasj* **60** (Feb., 2008) 111, [arXiv:0709.2467](#) [astro-ph].
- [110] M. Bursa, M. A. Abramowicz, V. Karas, and W. Kluźniak, “The Upper Kilohertz Quasi-periodic Oscillation: A Gravitationally Lensed Vertical Oscillation,” *apjl* **617** no. 1, (Dec., 2004) L45–L48, [arXiv:astro-ph/0406586](#) [astro-ph].
- [111] M. Bursa, “Global oscillations of a fluid torus as a modulation mechanism for black-hole high-frequency QPOs,” *Astronomische Nachrichten* **326** no. 9, (Nov., 2005) 849–855, [arXiv:astro-ph/0510460](#) [astro-ph].
- [112] M. Bursa, “High-frequency QPOs in GRO J1655-40: Constraints on resonance models by spectral fits,” in *RAGtime 6/7: Workshops on black holes and neutron stars*, S. Hledík and Z. Stuchlík, eds., pp. 39–45. Dec., 2005.
- [113] G. Török, K. Goluchová, J. Horák, E. Šrámková, M. Urbanec, T. Pecháček, and P. Bakala, “Twin peak quasi-periodic oscillations as signature of oscillating cusp torus,” *Mon. Not. Roy. Astron. Soc.* **457** no. 1, (2016) L19–L23, [arXiv:1512.03841](#) [astro-ph.HE].
- [114] E. Sramkova, G. Torok, A. Kotrlova, P. Bakala, M. Abramowicz, Z. Stuchlik, K. Goluchova, and W. Kluzniak, “Black hole spin inferred from 3:2 epicyclic resonance model of high-frequency quasi-periodic oscillations,” *Astron. Astrophys.* **578** (2015) A90, [arXiv:1505.02712](#) [astro-ph.HE].
- [115] J. Horak, “Weak nonlinear coupling between epicyclic modes in slender tori,” *Astron. Astrophys.* **486** (2008) 1, [arXiv:0805.2059](#) [astro-ph].
- [116] Z. Stuchlík and M. Kološ, “Models of quasi-periodic oscillations related to mass and spin of the GRO J1655-40 black hole,” *Astron. Astrophys.* **586** (2016) A130, [arXiv:1603.07366](#) [astro-ph.HE].
- [117] D. Tsang and D. Lai, “Corotational Damping of Diskoseismic C-modes in Black Hole Accretion Discs,” *Mon. Not. Roy. Astron. Soc.* **393** (2009) 992–998, [arXiv:0810.1299](#) [astro-ph].
- [118] W. Fu and D. Lai, “Effects of Magnetic Fields on the Diskoseismic Modes of Accreting Black Holes,” *Astrophys. J.* **690** (2009) 1386–1392, [arXiv:0806.1938](#) [astro-ph].
- [119] W. Fu and D. Lai, “Corotational Instability, Magnetic Resonances and Global Inertial-Acoustic Oscillations in Magnetized Black-Hole Accretion Discs,” *Mon. Not. Roy. Astron. Soc.* **410** (2011) 399, [arXiv:1006.3763](#) [astro-ph.HE].
- [120] Y. Avni, “Energy spectra of X-ray clusters of galaxies,” *Apj* **210** (1976) 642–646.

- [121] R. Shafee, J. E. McClintock, R. Narayan, S. W. Davis, L.-X. Li, and R. A. Remillard, “Estimating the spin of stellar-mass black holes by spectral fitting of the x-ray continuum,” *The Astrophysical Journal* **636** no. 2, (Dec, 2005) L113–L116. <https://doi.org/10.1086/498938>.
- [122] J. F. Steiner, R. C. Reis, J. E. McClintock, R. Narayan, R. A. Remillard, J. A. Orosz, L. Gou, A. C. Fabian, and M. A. P. Torres, “The Spin of the Black Hole Microquasar XTE J1550-564 via the Continuum-Fitting and Fe-Line Methods,” *Mon. Not. Roy. Astron. Soc.* **416** (2011) 941–958, [arXiv:1010.1013](https://arxiv.org/abs/1010.1013) [astro-ph.HE].
- [123] J. E. McClintock, R. Shafee, R. Narayan, R. A. Remillard, S. W. Davis, and L.-X. Li, “The Spin of the Near-Extreme Kerr Black Hole GRS 1915+105,” *Astrophys. J.* **652** (2006) 518–539, [arXiv:astro-ph/0606076](https://arxiv.org/abs/astro-ph/0606076).
- [124] J. F. Steiner, J. E. McClintock, and M. J. Reid, “The Distance, Inclination, and Spin of the Black Hole Microquasar H1743-322,” *Astrophys. J. Lett.* **745** (2012) L7, [arXiv:1111.2388](https://arxiv.org/abs/1111.2388) [astro-ph.HE].
- [125] M. Moscibrodzka, C. F. Gammie, J. C. Dolence, H. Shiokawa, and P. K. Leung, “Radiative Models of Sgr A* from GRMHD Simulations,” *Astrophys. J.* **706** (2009) 497–507, [arXiv:0909.5431](https://arxiv.org/abs/0909.5431) [astro-ph.HE].
- [126] J. M. Miller, C. S. Reynolds, A. C. Fabian, G. Miniutti, and L. C. Gallo, “Stellar-mass Black Hole Spin Constraints from Disk Reflection and Continuum Modeling,” *Astrophys. J.* **697** (2009) 900–912, [arXiv:0902.2840](https://arxiv.org/abs/0902.2840) [astro-ph.HE].
- [127] M. Middleton, C. Done, M. Gierliński, and S. W. Davis, “Black hole spin in GRS 1915+105,” *mnras* **373** no. 3, (Dec., 2006) 1004–1012, [arXiv:astro-ph/0601540](https://arxiv.org/abs/astro-ph/0601540) [astro-ph].
- [128] R. V. Shcherbakov, R. F. Penna, and J. C. McKinney, “Sagittarius A* Accretion Flow and Black Hole Parameters from General Relativistic Dynamical and Polarized Radiative Modeling,” *Astrophys. J.* **755** (2012) 133, [arXiv:1007.4832](https://arxiv.org/abs/1007.4832) [astro-ph.HE].
- [129] J. L. Blum, J. M. Miller, A. C. Fabian, M. C. Miller, J. Homan, M. van der Klis, E. M. Cackett, and R. C. Reis, “Measuring the Spin of GRS 1915+105 with Relativistic Disk Reflection,” *Astrophys. J.* **706** (2009) 60–66, [arXiv:0909.5383](https://arxiv.org/abs/0909.5383) [astro-ph.HE].
- [130] B. Aschenbach, “Mass and spin of the Sgr A* supermassive black hole determined from flare lightcurves and flare start times,” *memsai* **81** (Jan., 2010) 319.
- [131] B. S. Mills, S. W. Davis, and M. J. Middleton, “The black hole spin in GRS 1915+105, revisited,” *Astrophys. J.* **914** (2021) 6, [arXiv:2101.11655](https://arxiv.org/abs/2101.11655) [astro-ph.HE].
- [132] G. Fragione and A. Loeb, “An upper limit on the spin of SgrA* based on stellar orbits in its vicinity,” *Astrophys. J. Lett.* **901** no. 2, (2020) L32, [arXiv:2008.11734](https://arxiv.org/abs/2008.11734) [astro-ph.GA].
- [133] I. Banerjee, S. Chakraborty, and S. SenGupta, “Looking for extra dimensions in the observed quasi-periodic oscillations of black holes,” *JCAP* **09** (2021) 037, [arXiv:2105.06636](https://arxiv.org/abs/2105.06636) [gr-qc].
- [134] I. Banerjee, “Deciphering signatures of Bardeen black holes from the observed quasi-periodic oscillations,” *JCAP* **05** no. 05, (2022) 020, [arXiv:2201.00679](https://arxiv.org/abs/2201.00679) [gr-qc].

- [135] C. S. Reynolds, “The Spin of Supermassive Black Holes,” *Class. Quant. Grav.* **30** (2013) 244004, [arXiv:1307.3246 \[astro-ph.HE\]](#).